

## Investigation of Green Synthesized Silver Nanoparticles Using Aqueous Leaf Extract of *Artemisia Argyi* for Antioxidant and Antimicrobial Potentials

Anto Cordelia T A D<sup>1\*</sup>, Hng Huey Ping<sup>2</sup>

<sup>1</sup>Centre for Biodiversity Research, Faculty of Science, University Tunku Abdul Rahman (Perak Campus) Jalan Universiti, Bandar Barat, 31900 Kampar, Perak, Malaysia.

<sup>2</sup>Department of Chemical Science, Faculty of Science, University Tunku Abdul Rahman (Perak Campus) Jalan Universiti, Bandar Barat, 31900 Kampar, Perak, Malaysia.

Received: 14<sup>th</sup> Apr, 17; Revised 21<sup>st</sup> Aug, 17, Accepted: 14<sup>th</sup> Sept, 17; Available Online: 25<sup>th</sup> Dec, 17

### ABSTRACT

The current study employs green synthesis to acquire silver nanoparticles (AgNPs) using *Artemisia argyi* and appraise their antioxidant and antimicrobial potentials. AgNPs were synthesized using aqueous leaf extract of *Artemisia argyi* by sunlight irradiation. They were characterized using UV-visible spectrophotometer, FESEM, FTIR and XRD. The antioxidant capacity of AgNPs were evaluated using ABTS, DPPH, iron chelation, FRAP and NO radical scavenging methods. Antimicrobial activities of AgNPs were tested against *Escherichia coli* and *Staphylococcus aureus* using disc diffusion method. Descriptive statistical analysis was used to identify significant relationship between antioxidant activities of AgNPs. The synthesized AgNPs exhibited brown color light scattering and absorbed maximum wavelength of light at 450 nm. The synthesis of AgNPs was optimum at 0.01 M AgNO<sub>3</sub>. The green synthesized AgNPs were spherical in shape with size ranging from 16 nm to 32 nm. The FTIR analysis revealed the presence of proteins, phenolic and polar nitrile compounds in the AgNPs. The purified AgNPs possessed a face centered cubic structure with coexistence of silver chloride crystals. The total phenolic and flavonoid of AgNPs were found to be 77.45 mg GAE/g AgNPs and 205.29 mg GAE/g AgNPs respectively. The radical scavenging activity (EC<sub>50</sub>) showed highest activity for NO (31.33 µg/ml) followed by ABTS (128.82 µg/ml), DPPH (263.03 µg/ml) and Fe<sup>2+</sup> (1445.44 µg/ml) with a FRAP value of 1.22 mmol Fe<sup>2+</sup>/mg dry weight. AgNPs possessed inhibitory effect against both strains of bacteria in concentration dependent manner. This study discovered that green synthesized AgNPs using *Artemisia argyi* are promising sources of effective antioxidants and antimicrobial agents with a high surface area catalytic activity.

**Keywords:** *Artemisia argyi*, green synthesis, characterization, antioxidant activity, antimicrobial activity.

### INTRODUCTION

The nanotechnology is a big scale of nanometer size particles manufacturing, especially on metal based nanoparticles only of those between 1 to 100 nm in size<sup>1</sup>. The nanotechnology or nanoscience has been well known for some time. In 2000, United States National Nanotechnology Initiative (NNI) stands as worldwide pace for the nanotechnology projects. From the information in National Nanotechnology Initiative, it was first started by a physicist, the father of the nanotechnology known as Richard Feynman at 1959 on December 29 which explained his concept on the manipulation of atoms and molecules. The fundamental of nanoscale research was therefore based on a concept on which how the atoms or molecules could be controlled or manipulated. This was followed by Professor Norio Taniguchi which created the term 'Nanotechnology' in his book entitled, "Engines of Creation" at 1986 in describing the semiconductor processes at nanometer level. The research on nanotechnology projects contributes largely in nanoscale

electronic, optics, energy, environmental remediation and medical applications<sup>2</sup>. The nanotechnology was not only limited to electronic devices in daily life but they have also emerged into food industry and medicinal manufacturing area which uses nanoparticles as coating materials for antiseptic practices<sup>3</sup>.

Nanotechnology emerged as a new era in science and technology world when the microscopic instruments were built to enable the observation on the morphology and structure of the nanoscale particles<sup>2</sup>. These nanoparticles are of variety shapes and sizes. Such properties can be used to control and provide specific or enhanced effects on the applied products<sup>4</sup>. Currently, the synthesis of nanoparticles has developed from physical method to chemical method and from chemical method to biological method with the help of natural reducing compounds in living organisms<sup>5</sup>. Due the inconvenience caused by the machines usage in physical method and toxic by-products in chemical synthesis, the biosynthesis using fungi, microbes, algae and plants has been introduced for the more environmental

and cost effective production of nanoparticles<sup>6</sup>. Plants used in biosynthesis are of particular interest because it is faster and does not require selection from many species as in other living organisms. Currently, many extract from plants have been proven to possess the ability to reduce and stabilize the nanoparticles and this process is particularly known as green synthesis. Among the metal nanoparticles, silver nanoparticles were of interest in medical field as it was claimed to possess potential in antimicrobial activity against both strains of bacteria<sup>7</sup>. Studies also showed that the synthesis processes are affected by synthesis conditions which affect the outcome of nanoparticles<sup>8</sup>.

A few types of *Artemisia* plants have been studied to produce mostly spherical silver nanoparticles such as *Artemisia marshalliana*<sup>9</sup>, *Artemisia annua*<sup>4</sup>, *Artemisia nilagirica*<sup>10</sup>, *Artemisia capillaries*<sup>11</sup>, *Artemisia absinthium*<sup>12</sup> and *Artemisia vulgaris*<sup>13</sup> which is centered on the antibacterial activity in silver nanoparticles. Furthermore, the shapes of silver nanoparticles synthesized from these *Artemisia* species were reported to be mostly in spherical. Besides, the local *Artemisia argyi* extract has been found to possess remarkable content of flavonoid and phenolic compounds in its polar extracts<sup>14</sup>. These reducing compounds in *Artemisia argyi* are particularly potential towards the synthesis of silver nanoparticles. A few studies reported the binding of phytochemicals from plants onto the surface of nanoparticles contributed to the antioxidant activity in the silver nanoparticles<sup>15,16</sup>. Sunlight irradiation has also been used recently and proven the ability to induce the reduction process in the *Artemisia* plant<sup>4</sup>. Therefore, *Artemisia argyi* is selected for green synthesizing of silver nanoparticles through sunlight irradiation which may be a potential source of spherical shape nanoparticles, effective antioxidant agents and antimicrobial agents.

## MATERIALS AND METHODS

### Preparation of Plant Extract

To prepare the leaves extract, the dried leaves were first ground into powder using electric grinder. To prepare 10% *Artemisia argyi* aqueous extract, 25 g of *Artemisia argyi* leaves powder was weighted and was boiled in 250 ml of deionized water for 10 minutes. The boiled extract was left to cool at room temperature for 30 minutes and vacuum filtered to obtain the aqueous leaf extract of *Artemisia argyi*. The aqueous extract was kept in cool condition at 4 °C and was used within one week.

### Synthesis of Silver Nanoparticles

The preparation of silver nanoparticles from plant extract and silver nitrate was modified from Johnson and Obot<sup>4</sup>. A mixture of aqueous extract and 0.01M AgNO<sub>3</sub> in the ratio 1:9 was prepared by mixing 25 ml of aqueous extract in 225 ml of 0.01M AgNO<sub>3</sub>. The mixture was stirred evenly and reacted under direct sunlight for 10 minutes. The color changes were noted. The absorption spectrum of the silver nanoparticles solution was recorded from 300 nm to 800 nm using UV-Vis spectrophotometer (GENESYS 10).

### Characterization of Silver Nanoparticles

Silver nitrate solutions of 0.001 M, 0.005M, 0.01 M and 0.05 M were prepared from silver nitrate stock solution

(0.1M). 0.5 ml of 10% *Artemisia argyi* leaves extract was mixed into 4.5 ml of silver nitrate solution. The mixture was left under projector (5M) for 10 minutes and the absorption spectrum of the solution was recorded from 300 nm to 700 nm wavelength of light using UV-Vis spectrophotometer (GENESYS 10). The results were repeated in triplicates. The sample was scanned using field emission scanning electron microscope (JEOL USA JSM – 7610F) at magnification of 40,000X. The sample size was analyzed and calculated using Image J software. The disc was placed in the sample holder and the spectrum was run using FTIR spectrophotometer (Perkin- Elmer). The wavelength of absorbed light was recorded in cm<sup>-1</sup>. The presence of functional groups was interpreted. The lattice structure, crystalline phase, crystallite size and purity of silver nanoparticles from *Artemisia argyi* were analyzed using the continuous scan in X-Ray Diffractometer (Siemens D500) from 10° to 80° recorded at every 0.02° interval for 40.0 kV, 30.00 mA and scanning speed of 2.00 degree/min. The crystallite sizes were calculated using Scherrer equation.

### Total Phenolic Content (TPC)

Total phenolic content in silver nanoparticles was quantified by using Folin Ciocalteu (FC) method from Azlim Almey, et al.<sup>17</sup>. 100 µl of silver nanoparticles sample was mixed with 750 µl of 10% Folin-Ciocalteu reagent. The mixtures were left at room temperature for 5 minutes. Next, 750 µl of 6 % sodium carbonate (Na<sub>2</sub>CO<sub>3</sub>) was added into the mixture. The mixture of sample, Folin reagent and sodium carbonate mixture was left at room temperature for 2 hours. The absorbance was recorded at 725 nm using UV-Vis spectrophotometer (GENESYS 10). The test was repeated in triplicates and the total phenolic content of silver nanoparticles sample was expressed in gallic acid equivalent ± standard error using gallic acid standard curve.

### Total Flavonoid Content (TFC)

Total flavonoid content in silver nanoparticles was quantified by using method modified from Anto Cordelia, et al<sup>14</sup>. 150 µl of 5 % sodium nitrite (NaNO<sub>2</sub>) was added into 200 µl sample and the mixture was left at room temperature for 6 minutes. Next, 150 µl of 10% aluminum chloride (AlCl<sub>3</sub>) was added into each tubes and 800 µl of 10% sodium hydroxide (NaOH) solution was added into the mixture. The mixtures were left for 15 minutes at room temperature and the absorbance readings were taken at 510 nm using UV-Vis spectrophotometer (GENESYS 10). The triplicates of the data were obtained and the TFC was expressed in quercetin hydrate equivalent ± standard error using quercetin hydrate standard curve.

### 2,2'-azino-bis (3-ethylbenzothiazoline-6-sulphonic acid (ABTS) Radical Scavenging Activity Assay

1 ml of ABTS working solution was mixed into 100 µl of sample in the dark and the mixture was left for 10 minutes from a method modified from Wan, et al<sup>18</sup>. The absorbance measurement was taken at 734 nm using UV-Vis spectrophotometer (GENESYS 10). Ascorbic acid with working concentration from 0 µg/ml to 60 µg/ml was served as positive control. The ABTS scavenging ability was calculated in percentage inhibition (%).

Percentage inhibition (%) =  $(\text{Abs}_{\text{control}} - \text{Abs}_{\text{sample}} / \text{Abs}_{\text{control}}) \times 100\%$

#### **2,2-diphenyl-1-picrylhydrazyl (DPPH) Radical Scavenging Activity Assay**

The method in assessing the DPPH radicals scavenging activity of the silver nanoparticles samples was modified from Payne, et al.<sup>19</sup>. 1ml of 0.11 mM DPPH reagent was added into 200  $\mu\text{l}$  of sample or positive control and the solution was kept in dark for 60 minutes at room temperature (20 °C). The absorbance measurement was taken at 517 nm using UV-Vis spectrophotometer (GENESYS 10). The blank for DPPH assay was prepared by mixing 1 ml of methanol and 200  $\mu\text{l}$  of deionized water. The DPPH radical scavenging activity was calculated in percentage inhibition (%).

Percentage inhibition (%) =  $(\text{Abs}_{\text{control}} - \text{Abs}_{\text{sample}} / \text{Abs}_{\text{control}}) \times 100\%$

#### **Iron chelating Activity Assay**

The iron chelating ability of silver nanoparticles samples was measured according to the method modified from Jindal and Mohamad<sup>20</sup>. 30  $\mu\text{l}$  of ferrous chloride solution was added into 950  $\mu\text{l}$  of sample and positive control and the mixture was left in the dark for 16 hours. Then, 200  $\mu\text{l}$  of 5mM ferrozine was added and the mixture was allowed to stand at room temperature for 10 minutes. 1 ml of deionized water was added into each tube and the absorbance reading was taken at 562 nm using UV-Vis spectrophotometer (GENESYS 10). The assay was carried out in triplicates and the nitric oxide scavenging activity was calculated in percentage inhibition (%).

Percentage inhibition (%) =  $(\text{Abs}_{\text{control}} - \text{Abs}_{\text{sample}} / \text{Abs}_{\text{control}}) \times 100\%$

#### **Ferric Reducing Antioxidant Power (FRAP)**

The FRAP technique modified from Settharaksa, et al<sup>21</sup> was used to evaluate the reducing power of the silver nanoparticles. 2 ml of FRAP reagent was added to 200  $\mu\text{l}$  of silver nanoparticles and was left at 37 °C for 5 minutes. The assay was carried out in triplicates and the absorbance measurement was taken at 593 nm using UV-Vis spectrophotometer (GENESYS 10). Ferrous sulfate heptahydrate (0 to 0.40mM) was used as standard and the reducing power of sample was expressed in mM  $\text{Fe}^{2+}$  equivalent.

#### **Nitric Oxide (NO) Radical Scavenging Activity Assay**

The nitric oxide (NO) antioxidant assay used in previous study by Bhakya, et al.<sup>22</sup> was used as reference to evaluate the antioxidant activity of the silver nanoparticles. 200  $\mu\text{l}$  of 5.68 mM sodium nitroprusside was added into 800  $\mu\text{l}$  of silver nanoparticles sample and the mixture was irradiated under fluorescent light source at room temperature, 15 cm distance between the sample and light source. After 30 minutes, the mixture was removed from light source and 50  $\mu\text{l}$  of Griess reagent was added. The mixture was left for 10 minutes in the dark at room temperature. The assay was carried out in triplicates. The absorbance measurement was taken at 546 nm using UV-Vis spectrophotometer (GENESYS 10) and the nitric oxide scavenging activity was calculated in percentage inhibition (%).

Percentage inhibition (%) =  $(\text{Abs}_{\text{control}} - \text{Abs}_{\text{sample}} / \text{Abs}_{\text{control}}) \times 100\%$

#### **Antimicrobial Activity**

Gram negative *Escherichia coli* and Gram positive *Staphylococcus aureus* were selected in the evaluation of antimicrobial activity in silver nanoparticles. A working concentration of bacteria was standardized at  $0.500 \pm 0.02$  OD600. 10  $\mu\text{l}$  of silver nanoparticles (200  $\mu\text{g}/\text{ml}$ , 400  $\mu\text{g}/\text{ml}$ , 600  $\mu\text{g}/\text{ml}$ , 800  $\mu\text{g}/\text{ml}$ ) was placed on a piece of 5 mm Whatman filter paper and the paper was transferred onto the inoculated bacteria culture. The test was repeated by using positive control, antibiotic tetracycline at concentration of 50, 100 and 50  $\mu\text{g}/\text{ml}$ .

#### **Statistical Analysis**

The significant correlation between content of phenolic and flavonoid with the antioxidant activity of silver nanoparticles was assessed using correlation test. The experimental calculated percentage inhibition (%) in antioxidant assay and the calculated TPC (mg GAE/g) and TFC(mg QE/g) values were used as correlation coefficient data and significant level was set at  $P < 0.05$  (two-tailed). The significant difference for the growth inhibition of different bacteria species *Escherichia coli* (Gram negative) and *Staphylococcus aureus* (Gram positive) by silver nanoparticles and positive control was evaluated using a paired parametric t test. The experimental calculated average zone of inhibition (mm) was used as mean comparison between the bacteria species and the  $p < 0.05$  (two tailed) was set as significant level.

## **RESULTS AND DISCUSSION**

#### **Synthesis of Silver Nanoparticles**

The color change from yellow to dark brown was observed after 10 minutes of reaction which indicated the successful formation of silver nanoparticles. The maximum light absorption of dark brown color silver nanoparticles solution was detected at 450 nm. Similarly, the previous studies showed that the brown color formation and variation of light absorption peaks within 400 nm to 500 nm were formed due to the resonant frequency caused by the shape and size of the synthesized silver nanoparticles<sup>23,24,25</sup>. Together, these two features affirmed the successful conversion of silver nanoparticles from silver ions in accordance to their surface plasmon resonance principle.

#### **Characterization of Silver Nanoparticles**

**UV-Visible Spectrophotometer Analysis**  
As concentration of silver salts varies, the color intensity will also vary such that the increasing intensity of the brown color was spotted in the previous studies when the incubation time and concentration of silver nanoparticles increased<sup>25,26</sup>. Similar outcome was observed in terms of the increasing intensity of brown color from the use of 0.001 M and 0.005 M to 0.01 M silver nitrate. The increasing intensity of brown color indicated the increasing of silver nanoparticles been synthesized and this was due to the increasing silver ions in the mixture. The highly concentration silver nitrate caused a shift to shorter wavelength of light in the synthesized silver nanoparticles as analyzed from UV-Vis spectrophotometer.



Figure 1: The reaction of 10% *Artemisia argyi* and 0.01M silver nitrate solution before and after irradiation under sunlight. The mixture changes color from yellow (left) after incubation under direct sunlight for 10 minutes into dark brown solution (right). The absorption spectrum was recorded along 300 to 800 nm in UV-Vis spectrophotometer.

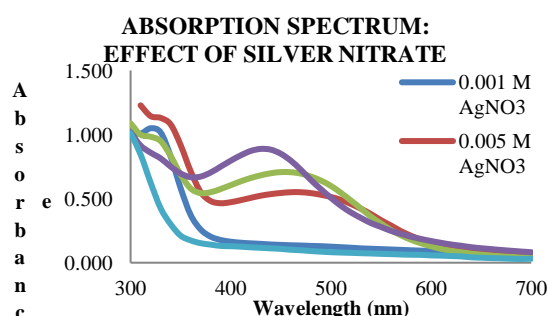
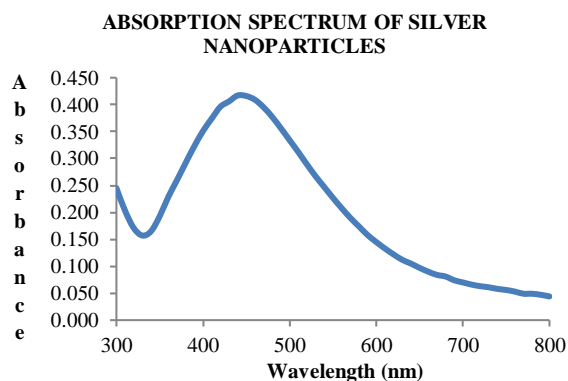
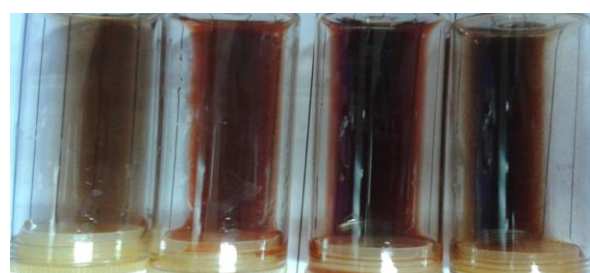


Figure 2: Effect of silver nitrate concentration on synthesis of silver nanoparticles.



Theoretically, the SRP is size and shape dependent in which the decreased in size will shift the wavelength to a shorter wavelength<sup>27,28</sup>. However, due to the presence of some unsuccessful coated nanoparticles when highly concentrated silver nitrate was been used which distorted the chemical reaction, the silver nanoparticles formed could have caused a shrink in their size and resulted in a shift to shorter wavelength in the resonant spectra.

#### FESEM Analysis

Field Emission Scanning Electron Microscope (FESEM) was used in the determination of the shape and size distribution of nanoparticles<sup>29,30</sup>. From the FESEM analysis, the silver nanoparticles were determined to be ranging from 16 nm to 32 nm with 31.97 nm average in size. The silver nanoparticles synthesized using *Artemisia argyi* by sunlight irradiation were also determined to be spherical in shape and free from agglomeration. The resonant frequency of these silver nanoparticles acted as the leading factor to the resonance spectra shown in the UV-Vis spectrophotometry analysis. The observed size and shape of these silver nanoparticles were related to the high reduction rate caused by the sunlight irradiation under the influence of phytochemicals composition from *Artemisia argyi* plant aqueous extract. Sunlight in combination with photon and heat energy could induce the reduction of silver ions by phytochemicals in plant extract into silver nanoparticles within short period of time therefore disallowing growth of larger particles. The previous studies also showed that the increase of temperature, providing higher energy had increased the rate of reduction in silver ions<sup>3,31</sup>. An earlier study using

*Artemisia* plant in synthesizing silver nanoparticles also showed that most of the synthesized silver nanoparticles were in spherical shapes<sup>3,10,32</sup>. Therefore, the factors such as concentration, nature and composition of phytochemicals compounds in *Artemisia argyi* with the help from sunlight irradiation were responsible for the formation of uniform spherical shape silver nanoparticles. These silver nanoparticles formed have a large surface area to volume and will be useful for size dependent catalytic reaction.

#### FTIR Analysis

Fourier Transform Infrared Spectroscopy (FTIR) was used to identify the biomolecules responsible for the synthesis of silver nanoparticles. The peak at  $3640\text{ cm}^{-1}$  was due to the amide functional group. The strongest absorption peak of the silver nanoparticles sample powder was detected at  $3422\text{ cm}^{-1}$  and  $2972\text{ cm}^{-1}$  represented the stretching vibration of hydroxyl group (-OH), amide (N-H) and alkanes group respectively. Sharp peaks were also detected at  $2371\text{ cm}^{-1}$ ,  $2345\text{ cm}^{-1}$  indicating stretch vibration of newly formed and existing  $\text{C}\equiv\text{N}$  bonds from plant extract. A strong and broad peak at  $1628\text{ cm}^{-1}$  represent the primary amines (C-N) that overlap the carbonyl stretch ( $\text{C}=\text{O}$ ) and aromatic  $\text{C}=\text{C}$  stretch. Peak at  $1400\text{ cm}^{-1}$  represent the aromatic  $\text{C}=\text{C}$  stretch in the compound while  $1260\text{ cm}^{-1}$  and  $1055\text{ cm}^{-1}$  represent the C-N (amines) stretching vibrations. From FTIR analysis, the functional groups such as hydroxyl group (-OH), alkane (C-H), nitriles ( $\text{C}\equiv\text{N}$ ), carbonyl group ( $\text{C}=\text{O}$ ), carboxylic acids (COOH), aromatic  $\text{C}=\text{C}$  stretch, amide (N-H) and amines ( $\text{NH}_2$ ) were used to affirm the presence of alcoholic, carboxylic,

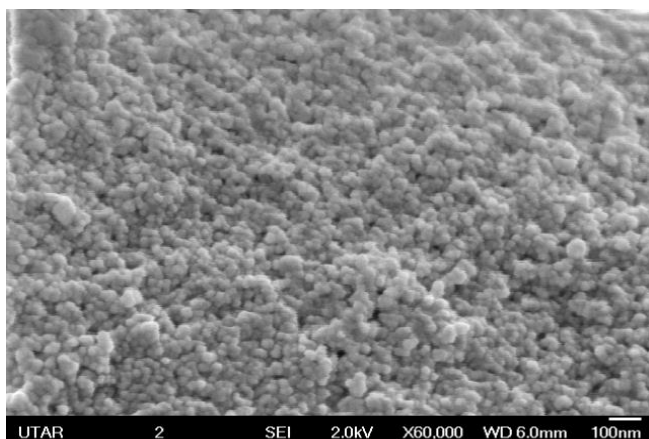


Figure 3: FESEM image analysis of silver nanoparticles at magnification of 40,000X.

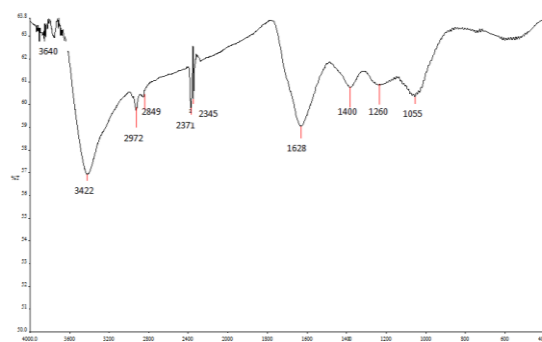


Figure 4: FTIR analysis of silver nanoparticles in freeze dried powder.

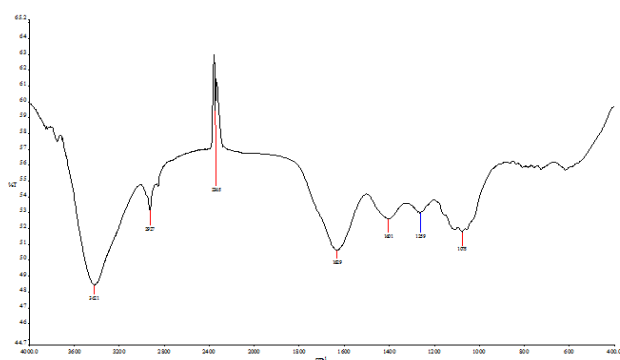


Figure 5: FTIR analysis of Artemisia argyi crude aqueous leaf extract.

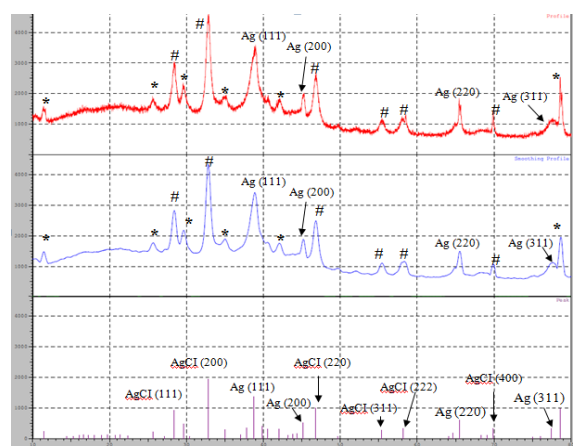


Figure 6: XRD spectra of silver nanoparticles. The detection of impurities were labeled as asterisk (\*) and secondary phase (#) in the profile and smoothing profile. Note that the peak profile was labeled with the planes of crystallite phase, Ag and secondary phase, AgCINPs.

Table 1: The total phenolic content and total flavonoid content in mg per g dry matter of silver nanoparticles powder using *Artemisia argyi*.

Bioactive compounds	Total phenolic content GAE equivalent	Total flavonoid content QE equivalent
Concentration of bioactive compounds (mg/g ± SE)	77.45 ± 0.75	205.29 ± 4.11

aromatic, amides, primary and aliphatic amines compounds in the silver nanoparticles.

As compared to the plant extract, silver nanoparticles showed functional groups of nearly identical except for amide and nitriles functional groups at 3640 and 2371 cm<sup>-1</sup>. The similar functional groups found between silver nanoparticles and plant extract substantiated that the functional groups detected in the silver nanoparticles were attributed to the phytochemical compounds from *Artemisia argyi* crude plant aqueous extract. The presence of alcohol groups in combination with the aromatic rings

and ketones groups determined the presence of the phenolic and flavonoid compounds in the plant extract which possessed the ability to reduce metal ions of silver (Ag<sup>+</sup>) into silver atoms (Ag<sup>0</sup>). The proteins from the plant extract stabilized the nanoparticles through protein ligand binding to the metal by various weak bonds such as hydrogen, ionic bonds, hydrophobic interaction or Van Der Waals interaction<sup>33</sup>. The detection of newly formed amide functional group also supported the formation of new protein bonds on the surface of silver nanoparticles as capping agents to further prevent the agglomeration of nanoparticles. As compared to other similar studies on silver nanoparticles, functional groups from both proteins and phenolic groups were detected as well which were claimed to be involved in the reduction and stabilization of silver nanoparticles synthesis<sup>26,34,35</sup>. The carbon-nitrogen bonds are polar bond, unlike alkynes, they can appear above 2200 cm<sup>-1</sup> as a stronger peak.

An earlier study of green synthesis of silver nanoparticles using apple extract suggested these nitrile compounds act as reducing and capping agents<sup>36</sup>. Besides, a chemical synthesis using stabilizing agent Trioctyl phosphine oxide



Table 2: The antioxidant capacity of silver nanoparticles from *Artemisia argyi* expressed in EC<sub>50</sub> (µg/ml) and FRAP value (mmol Fe<sup>2+</sup> equivalents/ mg dry weight).

Control /Sample	EC <sub>50</sub> values of radical scavenging activity ( µg/ml)				FRAP value*
	ABTS Scavenging	DPPH scavenging	Iron Chelating	NO Scavenging	
A.A	29.24 ± 0.02	18.71 ± 0.02	-	172.58 ± 0.01	10.32 ± 0.17
EDTA	-	-	11.02 ± 0.01	-	-
AgNPs	128.82 ± 0.02	263.03 ± 0.02	1445.44 ± 0.01	31.33 ± 0.03	1.22 ± 0.04

\* mmol Fe<sup>2+</sup> equivalents/ mg dry weight

Table 3: Statistical analysis of correlation coefficient in silver nanoparticles synthesized from 10% *Artemisia argyi* extract.

TOAC of Silver Nanoparticles	Total Phenolic content (TPC)		Total Flavonoid Content (TFC)	
	Correlation coefficient, r	P value	Correlation coefficient, r	P value
ABTS	0.9948	<0.0001 ****	0.9957	<0.0001 ****
DPPH	0.9184	0.0097 **	0.9189	0.0096 **
FRAP	0.9983	<0.0001 ****	0.9978	<0.0001 ****
Iron Chelating	0.9932	<0.0001 ****	0.9931	<0.0001 ****
NO	0.8985	0.006 **	0.9015	0.0055 **

P value <0.05 is set at significant \*\* highly significant \*\*\*\* excellently significant NS Not significant at 95%

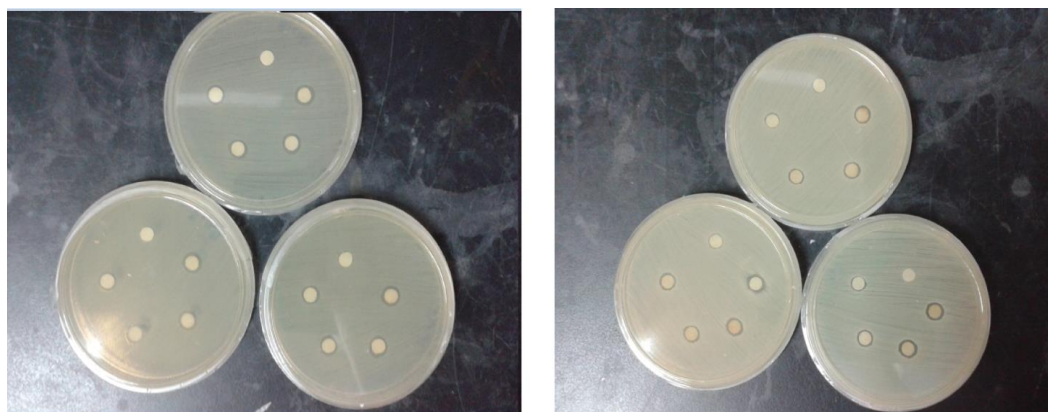


Figure 7: Antimicrobial disc diffusion test of silver nanoparticles.

Table 4: Zone of inhibition in antimicrobial activity of silver nanoparticles.

Concentration of AgNPs (mg/ml)	Zone of inhibition (mm)	
	<i>E.coli</i>	<i>S.aureus</i>
0	0	0
200	7.6 ± 0.1	6.7 ± 0.2
400	7.9 ± 0.2	7.3 ± 0.1
600	8.2 ± 0.2	7.7 ± 0.3
800	8.7 ± 0.3	8.3 ± 0.4

(TOPO) also showed a similar result<sup>37</sup>. In contrast, a chemical synthesis study using similar chemical synthetic reducing agent showed that the nitrile group was absent under the absence of stabilizing agents<sup>38</sup>. Therefore, the nitrile groups besides proteins were determined as part of stabilizing agents by contributing to the solubilization of silver nanoparticles in aqueous solvent. Moreover, the presence of polar nitrile groups also helped to explain the shift of light absorption to the short wavelength caused by highly concentrated silver nitrate during the formation of silver nanoparticles. The nitrile groups enabled the silver nanoparticles to acquire solubility in the solution in which

the malformed silver nanoparticles were able to disaggregate upon dilution. Therefore, phenolic, proteins and nitrile groups are responsible for reducing, capping and stabilizing the synthesized silver nanoparticles.

#### XRD Analysis

The pattern of the XRD peaks in the silver nanoparticles was evaluated based on the reference in JCPDS file No 04-0783. From the XRD result, the planes (111), (200), (220) and (311) reflected the face centered cubic structure of silver crystals. The average experimental lattice constant was determined to be 4.048 ± 0.018 Å as compared to the theoretical value of 4.085 Å in silver. The matching of lattice parameters and lattice constant determined the face centered cubic structure in the silver nanoparticles. The presence of secondary phase was identified to be the silver chloride crystallites as referred to the JCPDS file No.85-1355 corresponded to the planes (111), (200), (220), (311), (222) and (400) respectively. According to Zhu, Chen and Liu<sup>39</sup>, the formation of silver chloride was due to the oxidation of metallic silver by hydrogen peroxide and further undergone chlorination into silver chloride nanoparticles. The presence of chlorine elements was also confirmed by Energy Dispersive X-ray Spectroscopy (EDAX) analysis in previous studies proving similar

Table 5: Statistical analysis of antimicrobial test in silver nanoparticles.

Silver Nanoparticles	Paired parametric t test ( <i>E.coli</i> vs <i>S.aureus</i> )
Mean of differences $\pm$ SEM	0.600 $\pm$ 0.108
t- value	5.555
P-value	0.0115
Correlation coefficient, r	0.9922*

P < 0.05 was set as significant level \*effective significant pairing

results<sup>22,40,41</sup>. Minor impurities were also detected which could be caused by the crystallization of phytochemicals from plant extract. The size distribution of the silver nanoparticles was determined to be 7.63 nm, 14.38 nm, 14.44 nm and 7.56 nm at respective peaks from the Scherrer's equation with the average crystallite size of  $11.00 \pm 1.97$  nm.

#### Total Phenolic and Total Flavonoid Content

The phenolic and flavonoid compounds in the silver nanoparticles were determined to be  $77.45 \pm 0.75$  GAE mg/g and  $205.29 \pm 4.11$  QE mg/g respectively. When the content of these compounds in silver nanoparticles was compared to the previous study of local *Artemisia argyi* aqueous extract by Anto Cordelia, et al<sup>14</sup>, the concentration was found to have clearly increased. The silver nitrate and plant extract was added in 9:1 proportion which indicated that there is reduction in the amount of phytochemicals in the synthesized silver nanoparticles. However, instead of showing a lower total phenolic and flavonoid content, it was found to possess a higher total phenolic and flavonoid content than the crude plant extract. Besides, similar results were obtained in previous studies have also reported silver nanoparticles contained a higher phenolic and flavonoid content than the plant extract<sup>7,15,16</sup>. This could indicate that the antioxidant compounds expressed themselves better when adsorbed to the surface of silver nanoparticles for a more efficient complex formation between the functional groups from chemical reagents and antioxidant compounds.

#### Total Antioxidant Capacity of Silver Nanoparticles

Antioxidant assays of ABTS, DPPH, iron chelating, FRAP and NO scavenging were conducted in order to study the antioxidant capacity of the green synthesized silver nanoparticles using *Artemisia argyi* as reducing agent. The radical scavenging activity increased in order of: NO > ABTS > DPPH > Fe<sup>2+</sup> with a FRAP value of  $1.22 \pm 0.04$  mmol Fe<sup>2+</sup> /mg dry weight (EC<sub>50</sub> of AgNPs on scavenging radicals:  $128.82 \pm 0.02$   $\mu$ g/ml for ABTS;  $263.03 \pm 0.02$   $\mu$ g/ml for DPPH;  $1445.44 \pm 0.01$   $\mu$ g/ml for iron chelating;  $31.33 \pm 0.03$   $\mu$ g/ml for NO). A remarkable nitric oxide scavenging activity in silver nanoparticles was found in which  $31.33 \pm 0.03$   $\mu$ g/ml of the silver nanoparticles could successfully scavenge 50% of the nitric oxide radicals and was more effective than ascorbic acid. This might be due to the enhanced radicals scavenging rate of the synthesized silver nanoparticles in combination with instability of nitric oxide radicals and photon energy from light illumination. The explanation was also in agreement with Rodriguez-Gattorno, et al<sup>42</sup> which claimed that nitric oxide

can easily accept electrons from silver nanoparticles as it is relatively unstable due to the higher electronegativity on the nitric oxide radical. Correlation coefficient was used to study the relationship between the total phenolic and flavonoid content with the antioxidant capacity of the silver nanoparticles.

The antioxidant capacity in all the assays were found to significantly possess strong positive correlations with the total phenolic and total flavonoid content in the silver nanoparticles, highest in FRAP followed by ABTS, iron chelating, DPPH and least in NO scavenging. This correlation result reaffirmed that the antioxidant activity of silver nanoparticles were highly dependent on the content of phenolic and flavonoids compounds on their surfaces. The total antioxidant activity of the silver nanoparticles evaluated from the five antioxidant assays was enhanced in a concentration dependent manner as compared to the plant extract alone. This finding was proven by the comparison of the current result to the previous study of local *Artemisia argyi* plant extract by Anto Cordelia, et al.<sup>14</sup>. The enhancement of silver nanoparticles in antioxidant activity was first suggested by Patil and Kumbhar<sup>43</sup> through the preferential adsorption of antioxidant compounds onto the surface of the silver nanoparticles therefore causing an effective scavenging ability. However, instead of preferential adsorption, the enhanced antioxidant activity could be solely caused by the enhanced expression of antioxidant functional groups through the adsorption onto the metal surface of silver nanoparticles. This was supported by a similar FTIR peak pattern and intensity between the plant extract and the synthesized silver nanoparticles which indicated there is less likely the selective adsorption of antioxidant compounds occurred. The enhanced activity could also be attributed to the energy exchange between metals and adsorbed molecules caused by the cloud of delocalized electrons in providing the extra advantageous for hydrogen or electron bond breaking in antioxidant compounds. The energy transferring between metals and the molecules adsorbed on the surface was also mentioned in the electrical semi-conductive process by Egger, et al<sup>44</sup>. The enhancement of the antioxidant activity in silver nanoparticles was in the agreement with previous studies in which a remarkable amount of antioxidant compounds was found in the green synthesized silver nanoparticles which possessed a high antioxidant capacity for various radicals<sup>22,7,45</sup>.

#### Antimicrobial Activity of Silver Nanoparticles

The antimicrobial activity of silver nanoparticles was evaluated using Gram negative bacteria *Escherichia coli* and Gram positive bacteria *Staphylococcus aureus*. The exact mechanism of silver nanoparticles in antimicrobial activity is unclear and the main pathway was suggested by the releasing of silver ions and formation of free radicals that causes the inhibition of the protein synthesis and DNA replication<sup>46</sup>. The antimicrobial test showed that higher inhibitory effect against Gram-negative *Escherichia coli* than Gram positive *Staphylococcus aureus*. Nevertheless, Gram positive and Gram negative have different feature in their membrane such that thickness of peptidoglycan is

higher in Gram positive and lower in Gram negative bacteria. This explained that antimicrobial activity of silver nanoparticles was found to possess inhibitory effect against both bacteria strains with higher effectiveness on Gram negative *Escherichia coli* due to the thinner peptidoglycan layer in Gram negative cell wall as compared to Gram positive bacteria. Similar finding of higher inhibitory effect against Gram negative bacteria cells was also obtained in previous studies suggesting the involvement of silver ions released from silver nanoparticles in the antimicrobial mechanism of action<sup>4,24,30,34,40</sup>. Statistically, significant difference of  $0.600 \pm 0.108$  SEM mm and a significant correlation coefficient between the bacteria strains was established between the effectiveness of silver nanoparticles and antimicrobial activities concluded that the silver nanoparticles have a higher inhibition effect against Gram negative bacteria was highly dependent on the diffusion rate of silver ions through the bacterial cell membrane. In addition, the use of silver nanoparticles was claimed to be less reactive than silver ions which will be more suited for medical applications<sup>47</sup>. However, further investigation should be established to understand the related factors and silver ions releasing mechanism from silver nanoparticles.

## CONCLUSION

From the research, *Artemisia argyi* aqueous extract successfully synthesized the spherical shaped silver nanoparticles of size 16 nm to 32 nm through sunlight irradiation. The phytochemical content from *Artemisia argyi* aqueous extract under the irradiation of sunlight acted as good energy source by providing efficient reduction rate for the formation of the uniform and well distributed spherical shape silver nanoparticles. Concentration of silver nitrate should be in balance with the added plant extract. Silver nanoparticles were proven to possess face centered cubic crystalline structure with coexistence of silver chloride crystals and phytochemicals. The binding of phenolic and flavonoid compounds also caused the synthesized silver nanoparticles to adapt high and concentration dependent antioxidant capacity on ABTS, DPPH, iron chelating, FRAP and most effective in NO radicals. The green synthesized silver nanoparticles are potent antimicrobial agent on both Gram positive and Gram negative bacteria with higher affinity towards Gram negative bacteria. Based on the data obtained, we concluded that the green synthesized silver nanoparticles are potent antioxidant and antimicrobial agent which can be beneficial in medical applications and diseases treatment.

## ACKNOWLEDGEMENT

We would like to appraise our sincere gratitude to Universiti Tunku Abdul Rahman (UTAR) for providing sufficient equipments and facilities in completing the current study. We would also like to thank UTAR laboratory staff for their support and guidance during the conduct of this study.

## REFERENCES

- Hulla, J.E., Sahu, S.C. and Hayes, A.W., 2015. Nanotechnology: History and future. *Human and Experimental Toxicology*, 34(12), pp. 1318-1321.
- National Nanotechnology Initiative (NNI). 2000. "What is Nanotechnology?". [online] Available at: <<http://www.nano.gov/nanotech-101/what/definition>> [Accessed 2 January, 2017].
- Ahmed, S., Ahmad, M. and Swami, B.L. and Ikram, S., 2016. A review on plants extract mediated synthesis of silver nanoparticles for antimicrobial applications: A green expertise. *Journal of Advanced Research*, 7(1), pp. 17-28.
- Johnson, A. and Obot, I.B., 2014. Green synthesis of silver nanoparticles using *Artemisia annua* and *Sida acuta* leaves extract and their antimicrobial, antioxidant and corrosion inhibition potentials. *Journal of Materials and Environmental Science*, 5(3), pp. 899-906.
- Iravani, S., Korbekandi, H., Mirmohammadi, S.V. and Zolfaghari, B., 2014. Synthesis of silver nanoparticles: chemical, physical and biological methods. *Research in Pharmaceutical Sciences*, 9(6), pp. 385-406.
- Prabhu, S. and Poulouse, E.K., 2012. Silver nanoparticles: mechanism of antimicrobial action, synthesis, medical applications, and toxicity effects. *International Nano Letters*, 2(32), pp. 1-10. [online] Available at: <<https://link.springer.com/article/10.1186/2228-5326-2-32>> [Accessed 20 March 2017].
- Abdel-Aziz, M.S., Shaheen, M.S., El-Nekeety, A.A. and Abdel-Wahhab, M.A., 2013. Antioxidant and antibacterial activity of silver nanoparticles biosynthesized using *Chenopodium murale* leaf extract. *Journal of Saudi Chemical Society*, 18(4), pp. 356-363.
- Mansouri, S.S. and Ghader, S., 2009. Experimental study on effect of different parameters on size and shape of triangular silver nanoparticles prepared by a simple and rapid method in aqueous solution. *Arabian Journal of Chemistry*, 2(1), pp. 47-53.
- Salehi, S., Shandiz, S.A.S., Ghanbar, F., Darvish, M.R., Ardestani, M.S., Mirzaie, A. and Jafari, M., 2016. Phytosynthesis of silver nanoparticles using *Artemisia marschalliana* Sprengel aerial part extract and assessment of their antioxidant, anticancer, and antibacterial properties. *International Journal of Nanomedicine*, Vol. 11, pp. 1835-1846.
- Vijayakumar, M., Priya, K., Nancy, F.T., Noorlidah, A. and Ahmed, A.B.A., 2012. Biosynthesis, characterisation and anti-bacterial effect of plant-mediated silver nanoparticles using *Artemisia nilagirica*. *Industrial Crops and Products*, Vol. 41, pp. 235-240.
- Jang, H., Lim, S.H., Choi, J.S. and Park, Y., 2015. Antibacterial properties of cetyltrimethylammonium bromide-stabilized green silver nanoparticles against methicillin-resistant *Staphylococcus aureus*. *Archives of Pharmacal Research*, 38(10), pp. 1906-1912.
- Ali, M., Kim, B., Belfield, K.D., Norman, D., Brennan, M. and Ali, G.S., 2016. Green synthesis and characterization of silver nanoparticles using *Artemisia*



- absinthium* aqueous extract — A comprehensive study. *Materials Science and Engineering C*, 58(1), pp. 359-365.
13. Giri, K.R., Bibek, G.C., Kharel, D., and Subba, B., 2014. Screening of phytochemicals, antioxidant and silver nanoparticles biosynthesizing capacities of some medicinal plants of Nepal. *Journal of Plant Sciences*, 2(1), pp. 77-81.
  14. Anto Cordelia, T.A.D., Ti, W.M., Hnin, P.A. and Sam, J.H., 2016. Preliminary screening of *Artemisia argyi* for antioxidant potentials. *International Journal of Pharmacognosy and Phytochemical Research*, 8(2), pp. 347-355.
  15. Patra, J.K. and Baek, K.H., 2016. Green synthesis of silver chloride nanoparticles using *Prunus persica* L. outer peel extract and investigation of antibacterial, anticandidal, antioxidant potential. *Green Chemistry Letters and Reviews*, 9(2), pp. 132-142.
  16. Phull, A.R., Abbas, Q., Ali, A., Raza, H., Kim, S.J., Zia, M. and Haq, I., 2016. Antioxidant, cytotoxic and antimicrobial activities of green synthesized silver nanoparticles from crude extract of *Bergenia ciliata*. *Future Journal of Pharmaceutical Sciences*, 2(1), pp. 31-36.
  17. Azlim Almey, A.A., Ahmed Jalal Khan, C., Syed Zahir, I., Mustapha Suleiman, K., Aisyah, M.R. and Kamarul Rahim, K., 2010. Total phenolic content and primary antioxidant activity of methanolic and ethanolic extracts of aromatic plants' leaves. *International Food Research Journal*, Vol. 17, pp. 1077-1084.
  18. Wan, C.P., Yu, Y.Y., Zhou, S.R., Liu, W., Tian, S.G. and Cao, S.W., 2011. Antioxidant activity and free radical-scavenging capacity of *Gynura divaricata* leaf extracts at different temperatures. *Pharmacognosy Magazine*, 7(25), pp. 40-45.
  19. Payne, A.C., Mazzer, A., Clarkson, G.J.J. and Taylor, G., 2013. Antioxidant assays-consistent findings from FRAP and ORAC reveal a negative impact of organic cultivation on antioxidant potential in spinach but not watercress or rocket leaves. *Food Science & Nutrition*, 1(6), pp. 439-444.
  20. Jindal, H.M.K. and Mohamad, J., 2012. Antioxidant Activity of *Ardisia crispa* (Mata pelanduk). *Sains Malaysiana*, 41(5), pp. 539-545.
  21. Settharaksa, S., Madaka, F., Sueree, L., Kittiwisut, S., Sakunpak, A., Moton, C. and Charoenchai, L., 2014. Effect of solvent types on phenolic, flavonoid contents and antioxidant activities of *Syzygium Gratum* (Wight) S.N.. *International Journal of Pharmacy and Pharmaceutical Sciences*, Vol. 6 (2), pp. 114-116.
  22. Bhakya, S., Muthukrishnan, S., Sukumaran, M. and Muthukumar, M., 2016. Biogenic synthesis of silver nanoparticles and their antioxidant and antibacterial activity. *Applied Nanoscience*, 6(5), pp. 755-766.
  23. Shrivastava, S., Bera, T., Arnab Roy, A., Gajendra S., Ramachandrarao, P. and Dash, D., 2007. Characterization of enhanced antibacterial effects of novel silver nanoparticles. *Nanotechnology*, 18(22), pp. 1-9.
  24. Hussain, J.I., Kumar, S., Hashmi, A.A. and Khan, Z., 2011. Silver nanoparticles: preparation, characterization, and kinetics. *Advanced Materials Letters*, 2(3), pp. 188-194.
  25. Verma, A. and Mehata, M.S., 2015. Controllable synthesis of silver nanoparticles using *Neem* leaves and their antimicrobial activity. *Journal of Radiation Research and Applied Sciences*, 9(1), pp. 109-115.
  26. Ibrahim, H.M.M., 2015. Green synthesis and characterization of silver nanoparticles using banana peel extract and their antimicrobial activity against representative microorganisms. *Journal of Radiation Research and Applied Science*, 8(3), pp. 265-275.
  27. Mahmudin, L., Suharyadi, E., Utomo, A.B.S. and Abraha, K., 2015. Optical properties of silver nanoparticles for surface plasmon resonance (SRP)-based biosensor applications. *Journal of Modern Physics*, Vol. 6, pp. 1071-1076.
  28. Zhang, X.F., Liu, Z.G., Shen, W. and Curunathan, S., 2016. Silver nanoparticles: synthesis, characterization, properties, applications, and therapeutic approaches. *International Journal of Molecular Sciences*, 17(9), pp. 1534.
  29. Kalainila, P., Subha, V., Ravindran, E.R.S. and Renganathan, S., 2014. Synthesis and characterization of silver nanoparticles from *Erthrina indica*. *Asian Journal of Pharmaceutical and Clinical Research*, 7(2), pp. 39-43.
  30. Logeswari, P., Silambarasan, S., Abraham, J., 2012. Synthesis of silver nanoparticles using plants extract and analysis of their antimicrobial property. *Journal of Saudi Chemical Society*, 19(3), pp. 311-317.
  31. Amin, M., Anwar, F., Ramzan, M., Awais Iqbal, M., Rashid, U., 2012. Green synthesis of silver nanoparticles through reduction with *Solanum xanthocarpum* L. berry extract: characterization, antimicrobial and urease inhibitory activities against *Helicobacter pylori*. *International Journal of Molecular Science*, Vol. 13, pp. 9923-9941.
  32. Lim, S.H., Ahn, E.Y. and Park, Y., 2016. Green synthesis and catalytic activity of gold nanoparticles synthesized by *Artemisia capillaris* water extract. *Nanoscale Research Letters*, 11(1), pp. 474.
  33. Du, X., Xia, Y.L., Ai, S.M., Liang, J., Sang, P., Ji, X.L. and Liu, S.Q., 2016. Insights into protein–ligand interactions: mechanisms, models, and methods. *International Journal of Molecular Sciences*, 17(2), pp. 144.
  34. Allafchian, A.R., Mirahmadi-Zare, S.Z., Jalali, S.A.H., Hashemi, S.S. and Vahabi., 2016. Green synthesis of silver nanoparticles using *phlomis* leaf extract and investigation of their antibacterial activity. *Journal of Nanostructure in Chemistry*, 6(2), pp. 129-135.
  35. Jyoti, K., Baunthiyal, M. and Ajeet, S., 2016. Characterization of silver nanoparticles synthesized using *Urtica dioica* Linn. leaves and their synergistic effects with antibiotics. *Journal of Radiation Research and Applied Sciences*, 9(3), pp. 217-227.
  36. Ali, Z.A., Yahya, R., Sekaran, S.D. and Puteh, R., 2016. Green synthesis of silver nanoparticles using apple

- extract and its antibacterial properties. *Advances in Materials Science and Engineering*. [online] Available at: <<http://dx.doi.org/10.1155/2016/4102196>> [Accessed 2 March 2017].
37. Alagumuthu, G. and Kirubha, R., 2012. Synthesis and characterisation of silver nanoparticles in different medium. *Open journal of Synthesis Theory and Application*, Vol. 1, pp. 13-17.
  38. Tajdidzadeh, M., Azmi, B.Z., Mahmood Yunus, W.M., Abizin Talib, Z., Sadrolhosseini, A.R., Karimzadeh, K., Gene, S.A. and Dorraj, M., 2014. Synthesis of silver nanoparticles dispersed in various aqueous media using laser ablation. *The Scientific World Journal*. [online] Available at: <<https://www.hindawi.com/journals/tswj/2014/324921/cta/>> [Accessed 3 March 2017].
  39. Zhu, M.S., Chen P.L., Liu M.H., 2012. Highly efficient visible-light-driven plasmonic photocatalysts based on graphene oxide-hybridized one-dimensional Ag/AgCl heteroarchitectures. *Journal of Materials Chemistry*, 22(40), pp.21487 - 21494.
  40. Anandalakshmi, K., Venugobal, J. and Ramasamy, V., 2016. Characterization of silver nanoparticles by green synthesis method using *Pedaliium murex* leaf extract and their antibacterial activity. *Applied Nanoscience*, 6(3), pp. 399-408.
  41. Mahendran, G., Kumari R. B.D., 2016. Biological activities of silver nanoparticles from *Nothapodytes nimmoniana* (Graham) Mabb. fruit extracts. *Food Science and Human Wellness*, 5(4), pp. 207-218.
  42. Rodriguez-Gattorno, G., Diaz, D., Rendon, L. and Hernandez-Segura, G.O., 2002. Metallic nanoparticles from spontaneous reduction of silver (I) in DMSO. Interaction between nitric oxide and silver nanoparticles. *Journal of Physical Chemistry B*, 106(10), pp. 2482-2487.
  43. Patil, S.P. and Kumbhar, S.T., 2017. Antioxidant, antibacterial and cytotoxic potential of silver nanoparticles synthesized using terpenes rich extract of *Lantana camara* L. leaves. *Biochemistry and Biophysics reports*, Vol. 10, pp. 76-81.
  44. Egger, D.A., Liu, Z.F., Neaton, J.B. and Kronik, L., 2015. Reliable energy level alignment at physisorbed molecule-metal interfaces from density functional theory. *Nano Letters*, 15(4), pp.2448 -2455.
  45. Kumar, T.M., Christy, A.M.V., Ramya, R.C.S., Malaisamy, M., Sivaraj, C., Arjun, P., Raaman, N. and Balasubramanian, K., 2012. Antioxidant and anticancer activity of *Helicteres isora* dried fruit solvent extracts. *Journal of Academia and Industrial Research*, 1(3), pp. 148 -152.
  46. Malarkodi, C., Rajeshkumar, S., Paulkumar, K., Gnanajobitha, G., Vanaja, M. and Annadurai, G., 2013. Biosynthesis of semiconductor nanoparticles by using sulfur reducing bacteria *Serratia nematodiphila*. *Advances in Nano Research*, 1(2), pp. 83-91.
  47. Kim, J. Y., Sungeun, K., Kim J., Jongchan L. and Yoon, J., 2005. The biocidal activity of nano-sized silver particles comparing with silver ion. *Journal of Korean Society of Environmental Engineers*, 27(7), pp. 771-776.